LA-11352-MS

c.3

Initiation and Detonation
of Heterogeneous High Explosives:
A Unified Model

**High-Explosive
Grains**

δ_i

D_i

A_i

Los Alamos
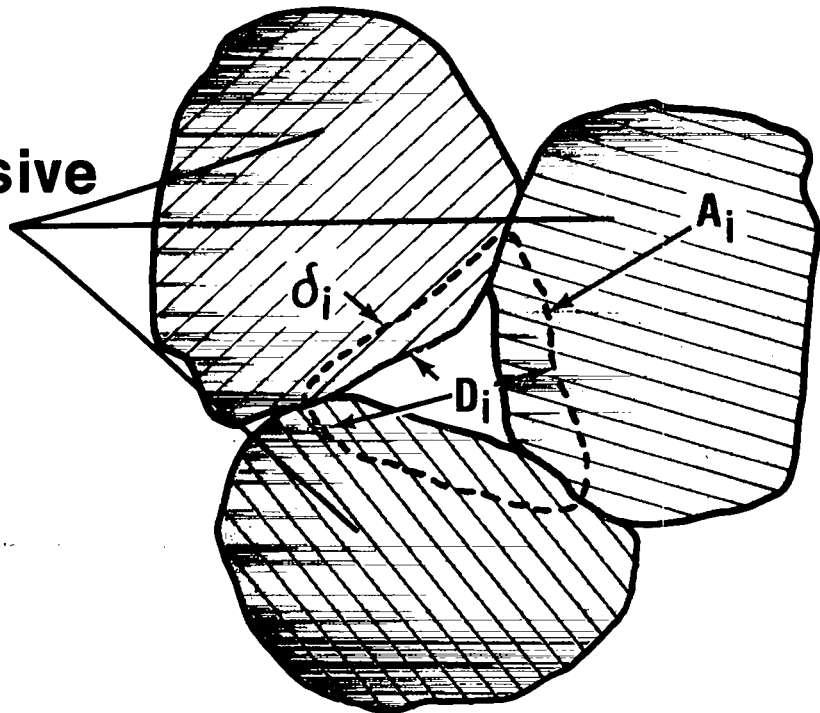
Cover figure: The principal high-explosive grains.
A_i = *hot-spot surface area;* δ_i = *shock-induced reaction zone thickness (exaggerated in figure);* D_i = *hot-spot characteristic length.*

Initiation and Detonation
of Heterogeneous High Explosives:
A Unified Model

Pier K. Tang

INITIATION AND DETONATION OF HETEROGENEOUS HIGH EXPLOSIVES: A UNIFIED MODEL

by

Pier K. Tang

ABSTRACT

Reaction processes in initiation and detonation of hetero-
geneous high explosives can be characterized by three dom-
inant rates that represent the special chemical and physical
features found in various stages of the reaction: hot spot,
propagation, and slow process. The first two stages con-
trol mainly the initiation; the last manifests itself in what
is known as the nonsteady detonation. Three principal rate
equations are thus constructed using the process time con-
cept. Examples with triaminotrinitrobenzene-based explo-
sives are presented to illustrate the model capability in the
simulations of initiation and detonation.

I. INTRODUCTION

Hydrodynamic calculations are routine in guiding designs of high-explosives sys-
tems. We are concerned with detonation and, most recently, initiation. A unified
model that can handle both phases without user intervention is not only of academic
interest but also of practical importance. An attempt had been made previously
to improve the detonation prediction by adding a slow-reaction component to a
model developed essentially for initiation.[1] Two-stage reaction was also included in
a different investigation, but no detail was given.[2] The approach presented in Ref.
1 lacks formalism; however, the necessary further refinement is the subject of this
investigation.

Initiation and detonation of high explosives (HE) involve many very complex
mechanical, thermal, and chemical processes, some of which defy description now.
However, characteristic times can be used to estimate the significance of the pro-
cess, regardless of the origin. In the simplest theoretical treatment, those times are
considered extremely short in comparison with the wave transit time and therefore

are ignored completely in hydrodynamic calculation. The consequence is a reaction model called programmed burn (Chapman-Jouguet burn), in which a constant detonation velocity is prescribed.

Initiation of HE, a nonsteady process, requires time and traveling distance for an initially weak shock, usually below Chapman-Jouguet (CJ) pressure, to develop into a detonation. Obviously, the time required for such a transition is due to some finite characteristic times in the initiation process. The need for a modeling approach without following strict first principles has been addressed elsewhere[3,4] and is not repeated here. Some areas of great interest in initiation applications have also been reported.[5,6,7]

In many HE systems, initiation involves only a small portion of the total system; the major part reaches the detonation state almost instantaneously. Unfortunately, we do not know *a priori* which part should be handled specially as initiation and which can be considered detonation only. The question remains of what to do with the high explosive after it is initiated and what should be used to describe the detonation behavior, generally believed to be a very fast process. Two recent studies indicate the need to consider a slow process near the end of reaction,[1,2] a process probably caused by slow and exothermic carbon clustering.[8] Because of that process, even the detonation cannot be regarded as very fast. The treatment of the slow process in Ref. 1 was handled *ad hoc* by switching the process time parameter from a high value to a lower one after the reaction reached a certain degree. The current paper improves on that procedure and places it on a better physical and mathematical foundation. A model containing both initiation and detonation features does not overlook the special characteristics of physics and chemistry in determining reaction rates for initiation as well as detonation and is definitely quite suitably applied because of the smooth transition from one phase to another.

II. THE MODEL

The heterogeneous nature of high explosives is well accepted, especially the concept of "hot spots," where a locally hot condition initiates decomposition much sooner. The mechanisms leading to local reaction include adiabatic compression, rapid shear, void collapse, friction, visco-plastic flow, and perhaps others. Although adiabatic compression can increase the internal energy and therefore raise the temperature in general, dissipation associated with the irreversible processes is even more effective in some highly local regions within the heterogeneous medium. The internal energy and subsequently the temperature in the hot spots become higher than that of the surroundings. Most heterogeneous high explosives consist of a main constituent, usually granular, and perhaps secondary explosive plus some binding materials. Figure 1 depicts such a configuration, with the principal high-explosive grains shown explicitly; the space between grains contains the rest and void. The hot spot, expected to occur near the surface of the grains, is where the dissipative process is most significant. The individual hot-spot volume is defined as the product of the hot-spot surface area, A_i, and the shock-induced reaction zone thickness, δ_i, the size of which is exaggerated in the illustration. Although the void concept

High-Explosive Grains
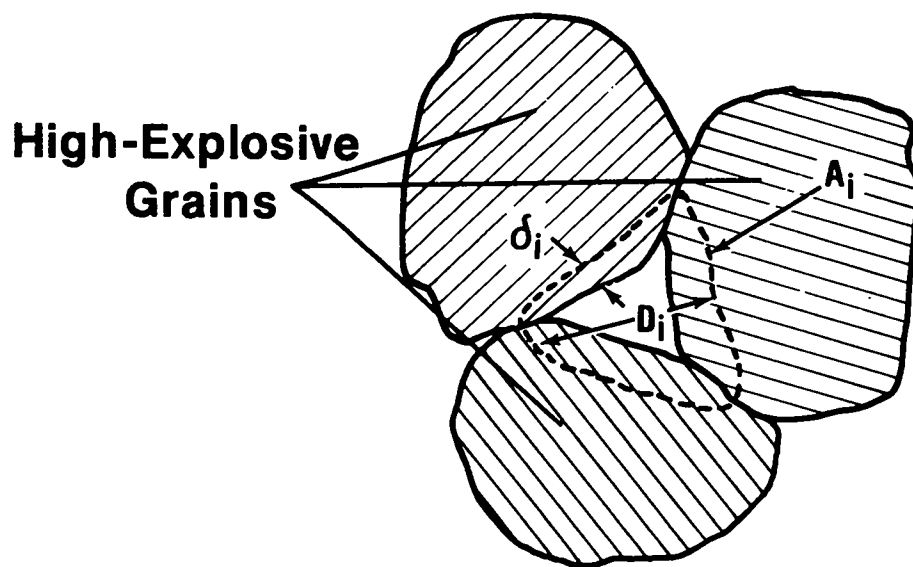
A_i: Hot-spot surface area

δ_i: Shock-induced reaction zone thickness

D_i: Hot-spot characteristic length

Fig. 1. Hot-spot region.

of hot spots is illustrated in the figure so that δ_i is confined within the grain, for other mechanisms δ_i can contain materials other than the principal explosive. The sum of all the hot-spot volumes per unit spatial volume, multiplied by the density ratio of the hot-spot zone ρ_h to the nominal one, ρ, results in

$$\eta = \frac{\rho_h}{\rho} \Sigma \, \delta_i A_i \ . \tag{1}$$

The hot-spot mass fraction, η, represents the fraction of the high explosive that is susceptible to the shock action. Clearly the total hot-spot surface area, ΣA_i per unit volume, must be related to a measurable quantity, known as the specific grain surface area, and is usually a small fraction of that quantity, depending on the degree of compaction and therefore density. The reaction zone thickness δ_i is related to the shock process, ignition threshold, and initial temperature. For now, η is treated as an empirical constant parameter and is typically a small number.

The third parameter in Fig. 1 is the characteristic length of the hot-spot region, D_i, which is associated with the void size. D_i must be related geometrically to the grain size and to loading conditions; it influences the dissipative mechanisms and therefore the hot-spot temperature.[9] The region exclusive of the hot spots is called the balance of explosive; its mass fraction is $(1-\eta)$. After the reaction in the hot-spot region has reached a certain intensity, the reaction will propagate into the balance of explosive.

3

The new treatment requires some repetition of earlier work.[1,4] Without undue explanation, the following major steps are suggested in the shock-induced reaction of heterogeneous high explosive.
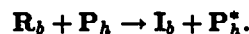
1. Hot-spot shock process leading to formation of intermediate state, a state of high temperature,
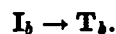
$$\mathbf{R}_h \rightarrow \mathbf{I}_h.$$
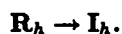
2. Hot-spot decomposition, consumption of intermediate state,

$$\mathbf{I}_h \rightarrow \mathbf{P}_h.$$
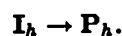
3. Heating of the balance of explosive by the hot-spot burned product, creation of the intermediate state for that region,

$$\mathbf{R}_b + \mathbf{P}_h \rightarrow \mathbf{I}_b + \mathbf{P}_h^*.$$

4. Decomposition of the intermediate in the balance of explosive, generation of transition products

$$\mathbf{I}_b \rightarrow \mathbf{T}_b.$$

The symbols $\mathbf{R}, \mathbf{I}, \mathbf{T}$, and $\mathbf{P}$ represent reactants, intermediates, transition products and final products; subscripts h and b are for hot spots and balance of explosives. $\mathbf{P}_h^*$ represents cooler $\mathbf{P}_h$ after energy transfer from the hot spots to the balance of explosive. The first two steps involve the hot spots only, but the last two control the burn in the balance of the explosive as a result of the hot-spot burn. This phase is called burn propagation. We say more about the transition products later.

Let us define R_h, I_h, T_h, and λ_h to be the component fractions of reactant, intermediate, transition product, and final product in the hot spots as the actual mass fractions divided by the hot-spot mass fraction η. A similar definition holds for R_b, I_b, T_b, and λ_b in the balance of explosive, and the respective mass fraction is $(1 - \eta)$.

With formulation similar to chemical kinetics, the time rates of change of those fractions of the hot spots for the processes given in steps 1 and 2 are

$$\frac{dR_h}{dt} = -\frac{R_h}{\tau_{sh}}, \tag{2}$$

$$\frac{dI_h}{dt} = \frac{R_h}{\tau_{sh}} - \frac{I_h}{\tau_h}, \tag{3}$$

and

4

$$\frac{d\lambda_h}{dt} = \frac{I_h}{\tau_h};$$

(4)

and of the balance of explosive in steps 3 and 4,

$$\frac{dR_b}{dt} = -\eta \frac{R_b}{\tau_e} \frac{(\lambda_h - f_o/\eta)}{(1 - f_o/\eta)},$$

(5)

and

$$\frac{dI_b}{dt} = \eta \frac{R_b}{\tau_e} \frac{(\lambda_h - f_o/\eta)}{(1 - f_o/\eta)} - \frac{I_b}{\tau_b}.$$

(6)

In the above rate equations, t is time; $\tau_{sh}, \tau_h, \tau_e$, and τ_b are the process times representing the shock process, hot-spot decomposition, energy transfer, and balance of explosive decomposition respectively; f_o is threshold of hot-spot burn.

Up to this point, the reaction steps and rate equations are almost identical to what were presented earlier except for introduction of a new component, the transition product, in the balance of explosive region. We recognize that although the chemical process in the balance of explosive is mainly decompositional, some recombinations would occur, particularly near the end of the reaction. A most prominent one is solid carbon coagulation (or condensation); the process is exothermic and slow.[8] The exothermic aspect allows us to include its contribution to the total reaction, but the process time can be quite long and cannot be ignored. Rather than accepting the decomposition products as final, we assume them to be transitional (or partially reacted), with two different kinds: one goes to the final product form rather quickly, but another takes considerably longer to reach the final state. The latter product includes, but is not necessarily limited to, the carbon products. Accordingly, we add two more steps:

5. Transition product becomes final product through fast reaction,

$$T_b \rightarrow P_f.$$

6. Transition product transforms into final product through slow reaction,

$$T_b \rightarrow P_s.$$

Subscripts f and s denote the fast and slow processes. We ignore the presence of the transition product and also the slow process in the hot spots caused by the small size and negligible amount of carbon products produced. Following steps 4 and 5, the rate equations are:

$$\frac{dT_{bf}}{dt} = \frac{I_b}{\tau_b} - \frac{T_{bf}}{\tau_f},$$

(7)

and

$$\frac{d\lambda_{bf}}{dt} = \frac{T_{bf}}{\tau_f},$$

(8)

5

and according to steps 4 and 6:

$$\frac{dT_{bs}}{dt} = \frac{I_b}{\tau_b} - \frac{T_{bs}}{\tau_s},$$ (9)

and

$$\frac{d\lambda_{bs}}{dt} = \frac{T_{bs}}{\tau_s},$$ (10)

where τ_f and τ_s are the characteristic times representing the fast and slow processes.

T_{bs} and λ_s are the actual mass fractions of the transition product and final product going through a slow process divided by a factor ζ and by $1-\eta$. T_{bf} and λ_f are defined in the same manner for the fast process, except the factor is $(1-\zeta)$. The factor ζ represents the fraction in the balance of explosive that would end up as carbon products or other products of slow reaction; it plays a similar role as the hot-spot mass fraction η in partitioning the energy as well as mass through two different branches of reactions. As we should expect, ζ is a small number.

Those fractions given in Eqs. (2) through (10) range in value from 0 to 1. They also obey the following relations through the definition of η:

$$R = \eta \, R_h + (1 - \eta)R_b,$$ (11)

$$I = \eta \, I_h + (1 - \eta) \, I_b,$$ (12)

$$T = (1 - \eta) \, T_b,$$ (13)

and

$$\lambda = \eta \, \lambda_h + (1 - \eta) \, \lambda_b;$$ (14)

and through ζ,

$$T_b = \zeta \, T_{bs} + (1 - \zeta) \, T_{bf},$$ (15)

and

$$\lambda_b = \zeta \, \lambda_{bs} + (1 - \zeta) \, \lambda_{bf}.$$ (16)

In addition, we have

$$R_h + I_h + \lambda_h = 1,$$ (17)

$$R_b + I_b + T_{bf} + \lambda_{bf} = 1,$$ (18)

and

$$R_b + I_b + T_{bs} + \lambda_{bs} = 1.$$ (19)

6

If those process times plus η, ζ, and f_o are known, the set of rate equations can be solved. Unfortunately, the system is quite complicated and the time parameters are yet undetermined. Extensive simplifications are necessary.

With some physical argument, first in the hot-spot region, the shock process is assumed to be much faster than the decomposition, so

$$\tau_{sh} \ll \tau_h. \tag{20}$$

The lifetime of J_s is very short; then J_s can be put to 0 and the rate process in that region can be reduced to a single equation:

$$\frac{d\lambda_h}{dt} = \frac{1}{\tau_h}(1 - \lambda_h). \tag{21}$$

In the balance of explosive, the effective energy transfer process is typically much slower than the decomposition, and that leads to

$$\tau_b \ll \tau_e/\eta. \tag{22}$$

Furthermore, we assume the fast process time τ_f be at most the same order as τ_b or even smaller; therefore, the lifetimes of both I_b and T_{bf} must be quite short. Again I_b and T_{bf} can be set to 0; then from Eqs. (18) and (19) we have

$$R_b = 1 - \lambda_{bf}, \tag{23}$$

and

$$T_{bs} = \lambda_{bf} - \lambda_{bs}. \tag{24}$$

Through Eqs. (5) and (10), the following equations are obtained:

$$\frac{d\lambda_{bf}}{dt} = \frac{\eta}{\tau_e}(1 - \lambda_{bf})\frac{(\lambda_h - f_o/\eta)}{(1 - f_o/\eta)}, \tag{25}$$

and

$$\frac{d\lambda_{bs}}{dt} = \frac{1}{\tau_s}(\lambda_{bf} - \lambda_{bs}). \tag{26}$$

Equation (25) is similar to Eq. (15) in Ref. 1 except that only the rate of final product from fast reaction is expressed here. It is important to notice that Eqs. (21) and (25) are the results of hot-spot and reaction propagation, whereas Eq. (26) is the consequence of slow reaction. Introducing the global mass fraction of slow process product, ψ, which is defined

$$\psi = (1 - \eta)\zeta,$$

we then have the total reaction fraction:

$$\lambda = \eta\lambda_h + \psi \, \lambda_{bs} + (1 - \eta - \psi)\lambda_{bf}, \tag{27}$$

where the three components λ_h, λ_{bf}, and λ_{bs} are controlled by the rates of Eqs. (21), (25), and (26). ψ is a small constant parameter.

7

We discuss various process times next. The hot-spot decomposition time τ_h is related to the shock state in that region. The passage of an initial shock wave of amplitude p_s produces an average hot-spot temperature θ_s given by

$$\theta_s = \theta_o \left[1 - m\frac{\theta_o}{\alpha}\ln\left(\frac{p_s}{p_o}\right)\right]^{-1},$$ (28)

where m, θ_o, and p_o are constant and α is the Arrhenius activation temperature. After the shock process, any further change of θ_s will be caused by the compression process:

$$\frac{d\theta_s}{dt} = \theta_s \Gamma \kappa \frac{dp}{dt},$$ (29)

with Γ being the Grüneisen coefficient and κ the isentropic compressibility. Both are assumed constant. Here $\frac{dp}{dt}$ is the time rate of pressure change.

For a given hot-spot temperature θ_s, there is an induction time of thermal explosion that we choose for the characteristic time τ_h:

$$\tau_h = \frac{\theta_s^2}{\alpha\beta Z}exp\left(\frac{\alpha}{\theta_s}\right).$$ (30)

In Eq. 30, β is the temperature coefficient resulting from chemical reaction and Z is the frequency factor for Arrhenius reaction. From now on we call τ_h the hot-spot process time since it contains the effects of shock and decomposition.

We now present the correlation of τ_e with the thermodynamic state. Since detailed knowledge is not available, we propose the following reasonable correlation:

$$\tau_e = [G_o\ p + G(p)]^{-1}.$$ (31)

The linear term in p represents the weaker energy transfer phase with constant G_o, but at higher pressure range, G is the dominant one. In fact, we have chosen that term with the pressure dependence to be that of Forest Fire rate,[4]

$$G(p) = exp\left(\sum_{i=o}^{n} a_i p^i\right),$$ (32)

where a_i's are constant.

Following the previous work,[1] the slow process is assumed independent of the hydrodynamic condition and, therefore, the slow process time τ_s is assumed constant.

IV. INITIATION

For a shock with intensity weaker than the CJ pressure, time and traveling distance are needed for that shock to evolve into a detonation wave as it propagates into the HE. The unique relation between the running distance and the imposing shock is known as a Pop plot, which forms the basis for construction of the Forest Fire rate. Conversely, a reaction model should be able to reproduce this result as part of the requirement in the simulation of initiation behavior.

Let us discuss the significance of those three principal rates. For convenience, we repeat those equations here.

$$\frac{d\lambda_h}{dt} = \frac{1}{\tau_h}(1 - \lambda_h), \tag{33}$$

$$\frac{d\lambda_{bf}}{dt} = \frac{\eta}{\tau_e}(1 - \lambda_{bf})\frac{(\lambda_h - f_o/\eta)}{(1 - f_o/\eta)}, \tag{34}$$

and

$$\frac{d\lambda_{bs}}{dt} = \frac{1}{\tau_s}(\lambda_{bf} - \lambda_{bs}). \tag{35}$$

They represent the three phases of reaction: hot spot, propagation, and slow process, respectively. In the initiation phase, both the shock pressure and the current pressure are usually low, so both the hot-spot process time τ_h and the energy transfer time τ_e as determined by Eqs. (28) to (32) are long in comparison with the wave transit time. The effective energy transfer time τ_e/η is even longer because of the small value of η. Depending on the initial shock strength, their values can be in the order of microseconds. The slow process time, τ_s, on the other hand, is about 100 ns and is therefore typically shorter than both τ_h and τ_e. We might even ignore the slow process stage by setting ψ to 0 without seeing significant reduction in run distance. Unless the initial shock is close to CJ value, much of Pop plot is not affected by the slow process. That is why we can simulate the initiation behavior quite well with consideration of the hot-spot and propagation processes only,[3,4] or we can conclude that a slow process involving a small amount of final products would not increase the run distance significantly. But from now on, we shall consider all three equations in our initiation calculation.

Initiation of high explosives is typically achieved by using a small detonator that usually sends out a shock wave of small area with short duration. With standard-size detonators, detonation can be obtained in the charge if the HE is sensitive enough, even in diverging configuration. Most Octogen (HMX)- and Hexogen (RDX)-based explosives can be initiated that way. However, initiation of insensitive high explosives (IHE) such as triaminotrinitrobenzene (TATB)-based materials requires a stronger push. A smaller detonator cannot meet this condition, so a booster is needed. The IHE can be made more sensitive by lowering the density and reducing the grain size[5,6] or by adding a more sensitive component such as pentaerthritol tetranitrate (PETN).[7]

Pop plot has been accepted to exemplify the initiation behavior of HE, so we show calculations of two TATB-based plastic-bonded explosives (PBX): PBX-9502 and X-0407, along with the experimental data. The widely investigated IHE, PBX-9502, contains 95% TATB and 5% chlorotrifluoroethylene/vinylidine fluoride copolymer (Kel-F 800). X-0407, by comparison, is more sensitive because its composition consists of 25% PETN, 70% TATB, and 5% Kel-F 800. Figure 2 shows the running distances versus the initial shock pressures for PBX-9502 and X-0407. Open markers are experimental data, curves are fittings of experiments, and filled markers are from calculations. X-0407 is much more sensitive than PBX-9502, particularly in the low-pressure region. The increased sensitivity of X-0407 is caused by the presence of PETN, and its chemical properties are used in the hot-spot process time calculation. The model capability of simulating the initiation behavior is thus proven.
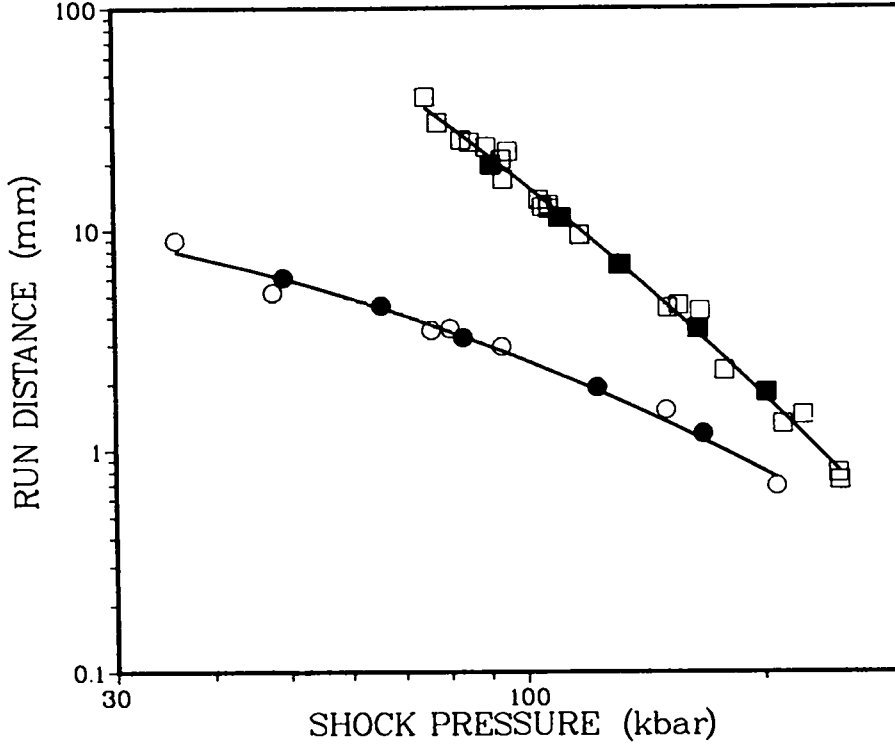
9

Fig. 2. Pop plots for PBX-9502 and X-0407: boxes for PBX-9502; circles for X-0407; open markers from experiments; curves for experimental fittings; filled markers from calculations .

V. DETONATION

We examine those reaction processes in detonation as given in Eqs. (33), (34), and (35). Since detonation takes place at high shock pressure level, the hot-spot process time τ_h must be quite short; the hot spots are consumed quickly, so $\lambda_h = 1$ quickly and Eq. (34) is greatly simplified.

$$\frac{d\lambda_{bf}}{dt} = \frac{\eta}{\tau_e}(1 - \lambda_{bf}). \tag{36}$$

Equation (36) becomes first-order, with the effective energy transfer time τ_e/η being quite small for high current pressure level; its value is about a few nanoseconds for a few explosives investigated so far. Since τ_s is typically around 100 ns, we have

$$\tau_e/\eta \ll \tau_s, \tag{37}$$

so $\lambda_{bf} \approx 1$; Eq. (35) effectively becomes

$$\frac{d\lambda_{bs}}{dt} = \frac{1}{\tau_s}(1 - \lambda_{bs}). \tag{38}$$

10

Equations (36) and (38) represent the asymptotic behavior of the original rate equations at detonation; they are equivalent to Eq. (18) with the rate switching conditions of Eqs. (20) and (21) in Ref. 1. In this formal treatment, we use three rates, Eqs. (33) through (35); all process times are accounted for, but Eq. (36) characterizes the fast reaction process whereas Eq. (38) controls the slow reaction process. We must recognize that the characteristic time in the fast reaction region is based on the Forest Fire rate; its accuracy is certainly questionable at high pressure because of very short run distances involved in wedge tests and the extrapolation of Pop plot data. The representation of the process by the energy transfer mechanism should also be modified because the chemical decomposition time τ_b might no longer be much shorter than the effective energy transfer time τ_e/η, as imposed by Eq. (22). However, the accuracy of τ_e/η will not affect the general outcome as long as Eq. (37) holds. Finally, the fraction of final products going through the slow process has been imposed through ψ.

Direct experimental technique with high precision has not been developed to investigate the detonation behavior interior of the HE charge. We use alternatives such as interface velocity record to infer the reaction process. Experiments were performed using a Fabry-Perot velocity interferometer to measure interface velocity between explosive and the polymethylmethacrylate (PMMA) window.[10] The systems were driven with a plane-wave lens, 25 mm of Composition B, and a layer of 10-mm aluminum. A thin aluminum foil (0.013 mm) was used to reflect the laser beam (Fig. 3). Increasing interface velocity histories with increasing explosive
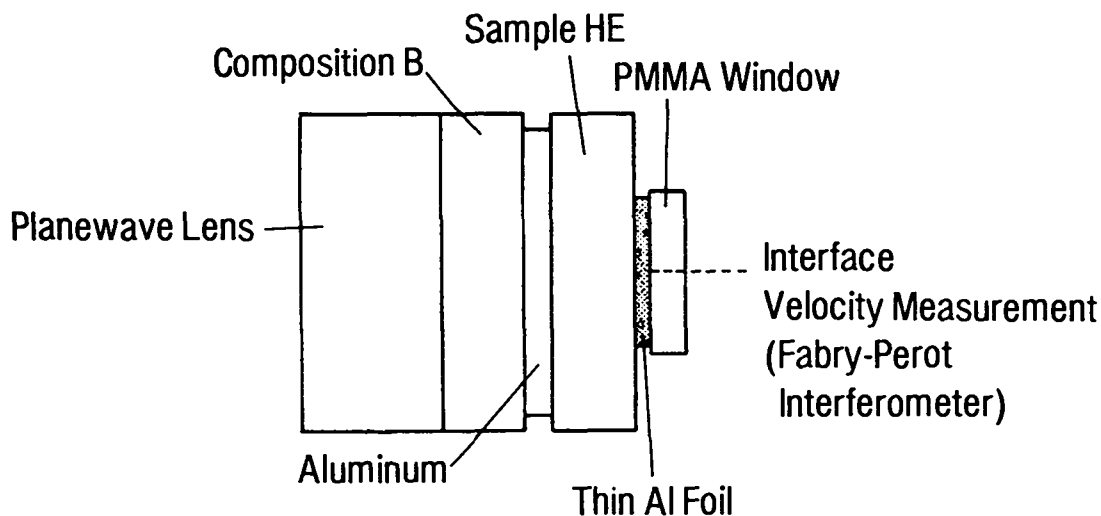

Fig. 3. Experimental setup for interface velocity between explosive and window.

charge lengths were observed for a class of TATB-based explosives, indicating non-steady detonation. The result of such experiments forms the basis of the earlier work, suggesting the existance of a slow process near the end of reaction in detonation.[1] The rate-switching technique is inadequate; the main goal of this new work is to overcome the deficiency.

The experimental results and calculations are presented in Figs. 4, 5, and 6 for PBX-9502 and Figs. 7, 8, and 9 for X-0407 with charge lengths of 13 mm, 25 mm, and 50 mm, respectively. The markers are from experiments and the curves are from calculations. $\psi = 0.2$ and $\tau_s = 75$ ns are used. The simulations match the experiments quite well in general except that the calculations show sharper peak at the detonation front. The peaks actually correspond to the von Neumann spikes that have been detected in separate experiments[11] for HMX-based explosives and in more recent work on both HMX- and TATB-based explosives.[2]. The von Neumann spikes are difficult to calculate accurately with a finite difference scheme and artificial viscosity in defining the shock region. Nevertheless, their existance is proven; the lack of such evidence in the experiments given in Ref. 10 is due mainly to the insufficient resolution.

We recall that the von Neumann spike corresponds to a purely unreacted state ($\lambda = 0$). As the reaction progresses, the fast reaction portion as determined by Eq. (36) is completed rather quickly, and the majority of the final products have reached their final state. The lifetime of the fast reaction is short but still finite and detectable. That is why in both calculation and experiments,[2,11] we observe this fast reaction zone and should not be surprised. Note that the lack of resolution in experiments does allow us to see the "effective" initial velocity increases with increasing HE charge length, a reflection of the effective C-J pressure. In calculation, the point corresponding to the end of the fast reaction represents the effective CJ condition. The ability of the model in the simulation of nonsteady detonation is therefore demonstrated.

VI. CONCLUSIONS

A model has been developed for the simulation of both initiation and detonation of heterogeneous high explosives. Using a building-block approach, we characterize each major stage with a process time of different physical and chemical origin. Those process times do not interact with each other significantly and therefore can be modeled separately. The advantages of this method are that explosives behavior can be realistically simulated within a single model and that a refinement in any particular area does not require substantial modification in others. For example, we can improve the hot-spot reaction to determine the temperature using a formal treatment such as given in Ref. 9 and, meantime, keep the propagation and the slow reaction parts as they are. Better definition of the fast reaction region can also be made by including the contribution from the decomposition without affecting the rest. New features can certainly be added using the process time concept within the existing framework of modeling.
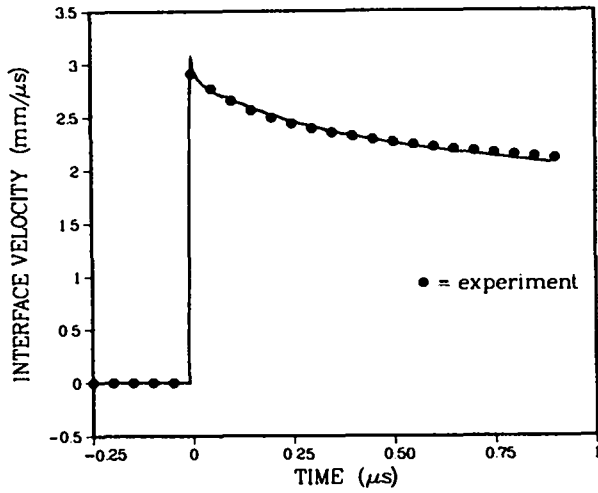
12

Fig. 4. Interface velocity between PBX-9502 and PMMA window, experiment vs calculation for 13-mm charge length.

Fig. 5. Interface velocity between PBX-9502 and PMMA window, experiment vs calculation for 25-mm charge length.
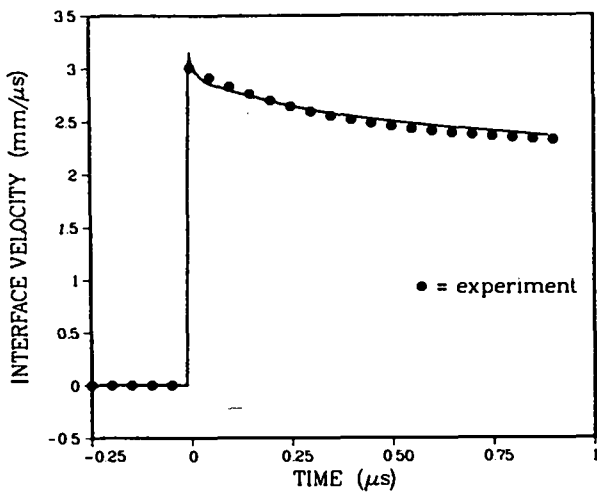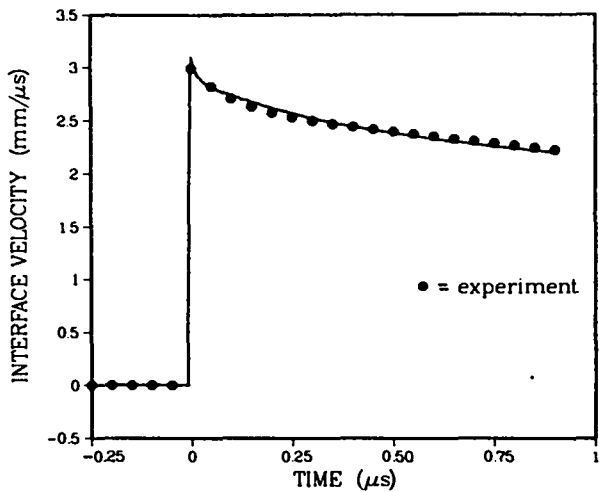

Fig. 6. Interface velocity between PBX-9502 and PMMA window, experiment vs calculation for 50-mm charge length.
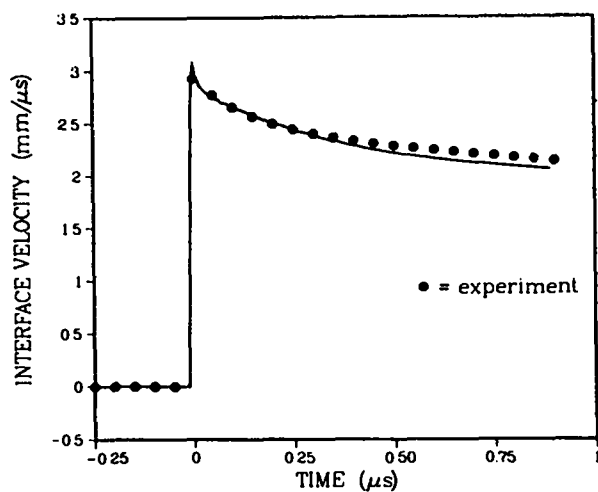
Fig. 7. Interface velocity between X-0407 and PMMA window, experiment vs calculation for 13-mm charge length.

Fig. 8. Interface velocity between X-0407 and PMMA window, experiment vs calculation for 25-mm charge length.
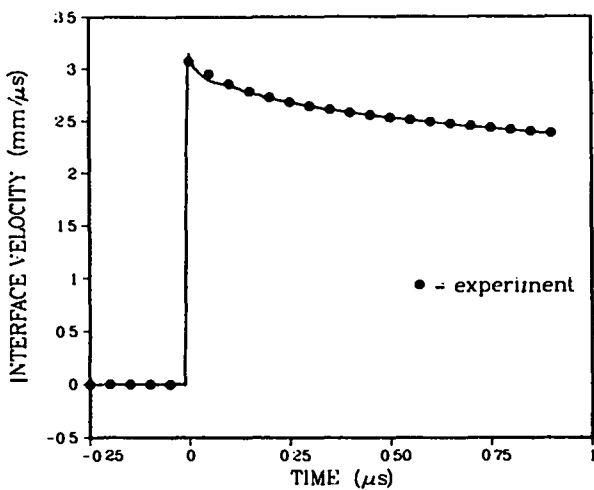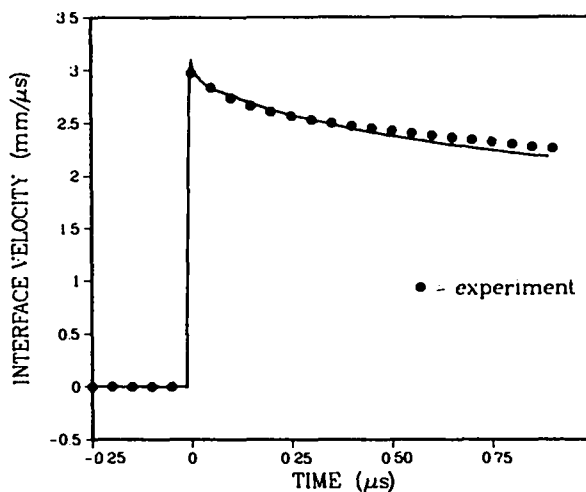

Fig. 9. Interface velocity between X-0407 and PMMA window, experiment vs calculation for 50-mm charge length.

14

ACKNOWLEDGMENT

REFERENCES

1. P. K. Tang, J. Appl. Phys. **63**, 1041 (1988).

2. C. M. Tarver, R. D. Breithaupt, and J. W. Kury in *Proceedings of the International Symposium on Pyrotechnics and Explosives*, (China Academic Publishers, Beijing, China, 1987), pp. 692-700.

3. J. N. Johnson, P. K. Tang, and C. A. Forest, J. Appl. Phys. **57**, 4323 (1985).

4. P. K. Tang, J. N. Johnson, and C. A. Forest, in *Proceedings of the Eighth Symposium (International) on Detonation*, (NSWC MP 86-194, Naval Surface Weapons Center, White Oak, MD, 1985), pp. 52-61.

5. P. K. Tang, C. A. Forest, J. N. Johnson, and W. L. Seitz, in *Proceedings of the International Symposium on Intense Dynamic Loading and Its Effects* (Science Press, Beijing, China, 1986), pp. 207-212.

6. P. K. Tang, Combustion and Flame **70**, 61 (1987).

7. P. K. Tang, in *Proceedings of the International Symposium on Pyrotechnics and Explosives* (China Academic Publishers, Beijing, China, 1987), pp. 687-691.

8. M. S. Shaw and J. D. Johnson, J. Appl. Phys. **62**, 2080 (1987).

9. R. B. Frey, U.S. Army Ballistic Research Laboratory technical report BRL-TR-2748, 1986.

10. W. L. Seitz, H. L. Stacy, and J. Wackerle, in *Proceedings of the Eighth Symposium (International) on Detonation*, (NSWC MP 86-194, Naval Surface Weapons Center, White Oak, MD, 1985), pp. 123-132.

11. D. Steinberg, and H. Chau, in *Proceedings of the Eighth Symposium (International) on Detonation*, (NSWC MP 86-194, Naval Weapons Surface Center, White Oak, MD, 1985), pp. 133-134.

Page Range	NTIS Price Code	Page Range	NTIS Price Code	Page Range	NTIS Price Code	Page Range	NTIS Price Code
001-025	A02	151-175	A08	301-325	A14	451-475	A20
026-050	A03	176-200	A09	326-350	A15	476-500	A21
051-075	A04	201-225	A10	351-375	A16	501-525	A22
076-100	A05	226-250	A11	376-400	A17	526-550	A23
101-125	A06	251-275	A12	401-425	A18	551-575	A24
126-150	A07	276-300	A13	426-450	A19	576-600	A25
						601-up*	A99

*Contact NTIS for a price quote.

Los Alamos Los Alamos National Laboratory
Los Alamos,New Mexico 87545